Combating Strong–Weak Spatial–Temporal Resonances in Time-Reversal Uplinks

Qinyi Xu, *Student Member, IEEE*, Yan Chen, *Senior Member, IEEE*, and K. J. Ray Liu, *Fellow, IEEE*

***Abstract*—In a time-reversal (TR) communication system, the signal-to-noise ratio (SNR) is boosted and the inter-user interference (IUI) is suppressed due to the spatial–temporal resonances, commonly known as the focusing effects, of the TR technique when implemented in a rich scattering environment. However, since the spatial–temporal resonances highly depend on the location-specific multipath profile, there exists a strong–weak spatial–temporal resonances effect. In the TR uplink system, different users at different locations enjoy different strengths of spatial–temporal resonances, i.e., the received signal-to-interference-noise ratios (SINRs) for different users vary, and the weak ones can be blocked from correct detection in the presence of strong ones. In this paper, we formulate the strong–weak spatial–temporal resonances in the multiuser TR uplink system as a max–min weighted SINR balancing problem by joint power control and signature design. Then, a novel two-stage adaptive algorithm that can guarantee the convergence is proposed. In stage I, the original nonconvex problem is relaxed into a Perron Frobenius eigenvalue optimization problem and an iterative algorithm is proposed to obtain the optimum efficiently. In stage II, the gradient search method is applied to update the relaxed feasible set until the global optimum for the original optimization problem is obtained. Numerical results show that our algorithm converges quickly, achieves a high energy-efficiency, and provides a performance guarantee to all users.**

***Index Terms*—Time Reversal, strong–weak spatial–temporal resonances, energy-efficiency, performance guarantee.**

I. Introduction

THE explosive growth of high speed wireless services that can support various wireless communication applications with a large number of users calls for future wideband communication solutions. Moreover, the dispersion of a channel in wideband communications will bring in an undesirable phenomenon: inter-symbol interference (ISI). Since the resolution of perceiving multiple paths increases significantly with the increase of bandwidth, ISI is more severe in a wideband single carrier system [1]. To tackle this problem, equalization techniques at the receiver side and/or multicarrier modulations are developed. While the performance of communication is improved, the complexity of terminal devices inevitably increases.

Manuscript received March 4, 2015; revised July 13, 2015; accepted August 19, 2015. Date of publication September 3, 2015; date of current version January 7, 2016. The associate editor coordinating the review of this paper and approving it for publication was Dr. Kaibin Huang.

The authors are with Origin Wireless, Inc., Greenbelt, MD 20770 USA, and also with the Department of Electrical and Computer Engineering, University of Maryland, College Park, MD 20742 USA (e-mail: qinyixu@umd.edu; yan@umd.edu; kjrliu@umd.edu).

Color versions of one or more of the figures in this paper are available online at http://ieeexplore.ieee.org.

Digital Object Identifier 10.1109/TWC.2015.2476457

On the other hand, thanks to its inherent nature that fully collects energy of multi-path propagation, the time-reversal (TR) based signal transmission is an ideal paradigm for low-complexity single-carrier broadband communication systems [2]. In essence, by treating each path of the multi-path channel in a rich scattering environment as a widely distributed virtual antenna, TR provides a high-resolution spatial-temporal resonance, commonly known as the focusing effect. This focusing effect indeed is the outcome of a resonance of electromagnetic field, in response to the environment, which concentrates energy propagated through the multipath channel onto a particular intended location at a specific time instant. The property of spatial focusing alleviates the inter-user interference (IUI) effectively in communications. Meanwhile, the traditional TR signature works as a matched filter at the access point (AP), which brings a temporal focusing and boosts the signal-to-noise ratio (SNR) at the intended location. In [3], a multi-user downlink system over multi-path channels using time reversal division multiple access (TRDMA) method was investigated. TRDMA is capable of achieving a very high diversity gain and of supporting low-cost and low-complexity terminal devices with only one single transmit antenna. As analyzed in [4], the TR-based wideband communication system was further proved to be a desired solution for future wireless communication systems. TR technique is also a promising solution for green Internet of Things (IoTs) in that a typical TR system has a potential of over an order of magnitude of reduction in power consumption and interference alleviation, as well as supporting heterogeneous terminal devices and providing an additional security and privacy guarantee [5]. However, the traditional TR signature is optimal only in the low symbol rate scenario due to ISI. A near optimal waveform design and power allocation solution was proposed in [6], suppressing both ISI and IUI and maximizing the achievable sum rate for the multiuser TRDMA downlink system.

The spatial-temporal resonance of the TR has been proposed as theory and validated through experiments in both acoustic domain and radio frequency (RF) domain. As verified in [7]–[9], energy of acoustic signal can be refocused with high resolution through a TR procedure after which a divergent wave issued from an acoustic source is converted into a convergent wave focusing on the source. This time-reversal mirror (TRM) is a self-adaptive technique that can be utilized to compensate for propagation distortions. The resonant effects of TR have also been validated through underwater acoustic experiments [10], [11]. In the RF domain, the TR spatial-temporal resonances of electromagnetic (EM) waves were studied in the SISO and MISO schemes and experiment results showed that

the quality of focusing is determined by the bandwidth frequency and spectral correlations of the field [12]. Lerosey *et al.* conducted experiments on microwaves in an indoor environment to further study the TR spatial-temporal focusing effects [13]. In [14], the TR technique was applied as a prefilter and its performance was investigated in the channel with large delay spread. Furthermore, the theory of TRM is formally developed for electromagnetic waves in [15]. However, since the quality of spatial-temporal resonances of EM waves highly depends on the propagation environment and transmission bandwidth, there exists a strong-weak spatial-temporal focsing effect in the multiuser TRDMA uplink system. Because of the strong-weak spatial-temporal resonances, the received SNRs of different users can be very distinct and weak signals can be blocked from correct detection in the presence of strong ones. Note that such a strong-weak spatial-temporal resonance is different from the well-known near-far effect in the CDMA uplink systems. For example, the TR resonances may bring in a signal boosting gain up to 6 - 10 dB while the near-far effect only causes attenuation in signal strength. Moreover, the reasons of creating the strong-weak spatial-temporal resonances is much more complicated than the near-far effect which is mainly resulted from the physical distances. The detailed differences between them will be discussed in the following.

The main reason causing the near-far problem in the CDMA uplink systems is that the distances from different transmitters to the same receiver differ a lot and the signals from the farther transmitters have lower SNR according to the inverse square law [16]. Dynamic power control algorithms have been proposed to alleviate the near-far effect in CDMA uplink systems and other cellular communication systems [17]–[21]. In [18], a centralized power adjustment scheme for cochannel interference control was proposed and investigated. Alpcan *et al.* formulated the distributed power control problem in CDMA system as a noncooperative game where a user-specific utility function based on SIR was designed and a quantitative criterion for admission control was derived upon possible equilibrium solutions [21]. Furthermore, as the usage of beamforming affected not only the individual link gains but also the power allocation strategy, joint optimization algorithms were proposed to enhance system performance [22]–[24]. With the uplink and downlink duality [25], [26], dynamical power control has also been applied to ensure multiuser fairness and to improve the total system data capacity in the downlink system [27]–[33]. The max-min criterion was first proposed in [27] for smart antenna downlink systems and the Perron Frobenius theorem [34], [35] was involved. Furthermore, a centralized algorithm was proposed in [28] for MISO downlink systems with frequency-flat channels. Recently, a nonlinear Perron Frobenius theorem has been introduced, and a distributed weighted proportional SINR algorithm was proposed to optimize multiuser downlinks [36]. The work has been extended to MIMO downlinks in [33], [37], and a power update problem under multiple power constraints was analyzed in [38]. However, the analysis and algorithms in the previous literature only considered optimizations in downlink systems where constraints are applied to the sum of individual powers. Compared to the total power constraints, to address the nonconvex max-min optimization under multiple individual power constraints is more complicated. Moreover, most of existing literature considered the frequency-flat channel model or multi-carrier systems and thus the inter-symbol interference (ISI), which is an important issue in the single-carrier system, has been omitted in the analysis.

Unlike the CDMA near-far problem resulted solely from distance, the TRDMA uplink systems suffer from the strong-weak spatial-temporal resonances among different users mainly due to the different resonances resulted from location-specific multipath environments. The performance of each link depends on the corresponding signal-to-interference-noise ratio (SINR). To guarantee the performance, we need to combat the strong-weak spatial-temporal resonances and to balance the SINRs among all links. To this end, we formulate the strong-weak spatial-temporal resonances combating problem in the TRDMA uplink system as a max-min weighted SINR optimization problem by the means of joint power allocation and signature filter design. Note that such a problem is non-convex and has many individual constraints which make it even harder to handle. To tackle this challenge, in this work, we propose a two-stage algorithm that solves this problem efficiently in two steps and converges to the global optimum quickly. In stage I, the original optimization problem is relaxed into a Perron Frobenius eigenvalue optimization problem by converting all the individual power constraints into a total power constraint. An iterative algorithm is proposed that is targeted to tackle the relaxed problem. In stage II, in order to find the global optimum for the original problem, the gradient search method is applied to shrink the relaxed feasible set. Simulation results demonstrate that the proposed algorithm is capable of providing a performance guarantee to all users regardless of their channel gains. Furthermore, our proposed algorithm is highly energy efficient comparing to the Basic TR schemes [3].

This paper is organized as follows. In Section II, the system model and problem formulation is described. In Section III, we relax the original TRDMA uplink SINR balancing problem with individual power constraints into an eigenvalue optimization problem and introduce an iterative algorithm which alternately optimizes signature matrix and power assignment vector. The two-stage adaptive algorithm for the TRDMA uplink SINR balancing problem with individual constraints is proposed in Section IV. Finally, numerical simulation in Section V demonstrates the performance improvement of our proposed scheme compared with traditional methods and conclusion is drawn in Section VI.

II. System Model

As shown in Fig. 1, in this work, we consider a TRDMA uplink system, where K users transmit data through the same media to one single access point (AP) simultaneously. In conventional single-carrier uplink systems, there is a detectability problem where signals with strong SNRs block weaker signals from being detected, e.g. the well-known near-far effect in the CDMA uplink system [1]. In CDMA uplink systems, the difference between SNRs of received signal is caused by the variations in transmit power and distance-based propagation attenuation. In the TRDMA uplink system, however, besides

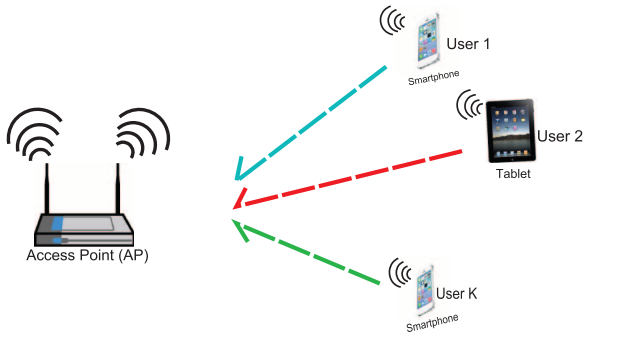

Fig. 1. Representative case for TRDMA uplink system.

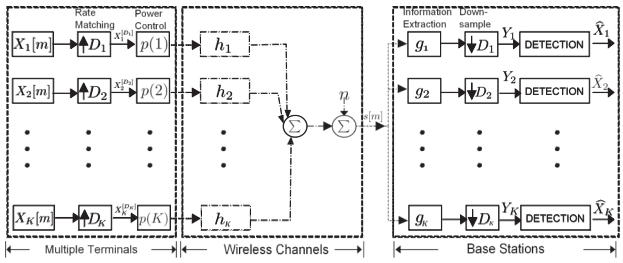

Fig. 2. Diagram for TRDMA uplink system.

the variations in transmit power and distance-based pathloss, the multipath channel gain brings in the strong-weak spatial-temporal resonances that cause the SNRs of the received signals to be different. Therefore, the detectability problem also commonly exists in the TRDMA uplink systems and needs to be carefully addressed.

The schematic diagram of a TRDMA uplink system is shown in Fig. 2 [5]. We can see that the signal of k^{th} user, X_k, is first upsampled by a backoff factor D_k. Then, the upsampled signal $X_k^{[D_k]}$ is boosted by a power control factor $p(k)$ before being transmitted through the location-specific multipath channel h_k. Since all the transmitted signals from different users are combined over the air, the received signal at the AP is a mixture of all transmitted signals and noise. To extract the information of different users, the received signal passes through a user-specific signature filter bank $\mathbf{g}_i$ which is designed according to the channel information obtained in the channel probing phase. In the channel probing phase, devices send an impulse or a pseudorandom noise (PN) sequence to the AP [2], such that the channel estimation can be obtained. We found through real experiments that channel response is rather stationary. In order to combat variations on channels and number of users, TR communication systems must rely on the channel probing phase to update the channel information frequently. This can be done really quick to be unnoticeable to users under time-varying situation. Then the output is downsampled by a backoff rate D_i, and a series of detectors are performed to detect the information of each user.

However, since the multipath channel gains vary among different users, the SINR of each user in the received signal may be different, and consequently the information of some users may not be detected correctly. From Fig. 2, we can see that, for a fixed detector, the received SINRs of users are determined jointly by the power control factor and the signature filter. Therefore, in this work, our objective is to jointly optimize signature $\mathbf{G} = [\mathbf{g}_1, \ldots, \mathbf{g}_K]$ and power allocation $\mathbf{p} = [p(1), \ldots, p(K)]^T$ to make sure the information of all users can be correctly detected.

A. Problem Formulation

Now, let us take a close look at this strong-weak spatial-temporal resonances problem and formulate it into an optimization problem. According to the system diagram in Fig. 2, the received signal at the AP can be written as follows

$$s[m] = \sum_k \sum_l \sqrt{p(k)} h_k[m-l] X_k^{[D_k]}[l] + n[m], \quad (1)$$

where $X_k^{[D_k]}$ is the upsampled version of the transmitted signal from the k^{th} user, $p(k)$ is the transmit power and h_k denotes the channel impulse response of the k^{th} user to AP with channel length L_k, i.e., $h_k[m] = 0$ for $m < 0$ and $m > L_k - 1$.

The (1) can be rewritten in a matrix form as $\mathbf{s} = \sum_k \sqrt{p(k)} \mathbf{H}_k \mathbf{x}_k^{[D_k]} + \mathbf{n}$, where $\mathbf{s}$ is a $(2L-1) \times 1$ vector with $L = max_k\ L_k$, $\mathbf{H}_k$ is a $(2L-1) \times L$ Toeplitz matrix with each column being the shifted version of $\mathbf{h}_k$, and $\mathbf{n}$ denotes the additive white Gaussian noise (AWGN) vector whose elements are identical complex Gaussian with mean zero and variance σ^2.

At the AP side, the received signal $\mathbf{s}$ first passes through a user-specific signature filter bank $\{\mathbf{g}_i, \forall i\}$ to extract information and to suppress interference. Then it is downsampled to obtain Y_i as follows

$$\begin{aligned} Y_i[m] &= \sum_{j=1}^{K} \sum_l \sqrt{p(j)} X_j[l](h_j * g_i)[mD_i - lD_j] + n[m] \\ &= \sqrt{p(i)} X_i[m](h_i * g_i)[0] \\ &\quad + \sqrt{p(i)} \sum_{l=-\lfloor \frac{L-1}{D_i} \rfloor \neq 0}^{l=\lfloor \frac{L-1}{D_i} \rfloor} X_i[m-l](h_i * g_i)[D_i l] \\ &\quad + \sum_{j \neq i} \sqrt{p(j)} \sum_{l=-\lfloor \frac{L-1}{D_j} \rfloor}^{l=\lfloor \frac{L-1}{D_j} \rfloor} X_j[m-l](h_j * g_i)[D_j l] + \tilde{n}_i[m], \end{aligned} \quad (2)$$

where $\tilde{n}_i$ is a downsampled version of $n * g_i$.

Based upon (2), the uplink SINR for user i is given as,

$$SINR_i^{UL}(\mathbf{G}, \mathbf{p}) = \frac{p(i) \mathbf{g}_i^H \mathbf{R}_i^{(0)} \mathbf{g}_i}{p(i) \mathbf{g}_i^H \hat{\mathbf{R}}_i \mathbf{g}_i + \sum_{j \neq i} p(j) \mathbf{g}_i^H \mathbf{R}_j \mathbf{g}_i + \sigma^2}, \quad (3)$$

where $\mathbf{G} = [\mathbf{g}_1, \ldots, \mathbf{g}_K]$ is the signature matrix, $\mathbf{p} = [p(1), \ldots, p(K)]^T$ is the power allocation vector, $\mathbf{R}_i^{(0)} = \mathbf{H}_i^{(L)H} \mathbf{H}_i^{(L)}$ with $\mathbf{H}_i^{(l)}$ being the l^{th} row of $\mathbf{H}_i$ and the superscript H denoting the hermitian operator, $\mathbf{R}_j = \tilde{\mathbf{H}}_j^H \tilde{\mathbf{H}}_j$,

$\tilde{\mathbf{H}}_j$ is the upsampled version of $\mathbf{H}_j$ with factor D_j and sampling center located at $\mathbf{H}_j^{(L)}$, and $\hat{\mathbf{R}}_i = \mathbf{R}_i - \mathbf{R}_i^{(0)}$. The first two terms in the denominator, $p(i)\mathbf{g}_i^H\hat{\mathbf{R}}_i\mathbf{g}_i$ and $\sum_{j\neq i} p(j)\mathbf{g}_i^H\mathbf{R}_j\mathbf{g}_i$, represent ISI and IUI respectively.

Let us define a crosstalk matrix $\mathbf{\Phi}$ for the TRDMA uplink system whose elements correspond to the ISI and IUI term in $SINR_i^{UL}$ as $[\mathbf{\Phi}]_{ij} = \begin{cases} \mathbf{g}_j^H\mathbf{R}_i\mathbf{g}_j, & i \neq j \\ \mathbf{g}_i^H\hat{\mathbf{R}}_i\mathbf{g}_i, & i = j \end{cases}$. The crosstalk matrix $\mathbf{\Phi}$ is of all positive components, and $\mathbf{\Phi}_i$ is the i^{th} column of matrix $\mathbf{\Phi}$.

Moreover, $\mathbf{D}$ is defined as a diagonal matrix with $[\mathbf{D}]_{ii} = \gamma_i/\mathbf{g}_i^H\mathbf{R}_i^{(0)}\mathbf{g}_i$, and γ_i is the SINR weighted factor for i^{th} user which supports heterogeneous SINR requirements. Then we can have $SINR_i^{UL}(\mathbf{G}, \mathbf{p})/\gamma_i = p(i)/[\mathbf{D}]_{ii}(\mathbf{\Phi}_i^T\mathbf{p} + \sigma^2)$,

In order to ensure the fairness among all users and to boost the system performance, we jointly design the signature matrix $\mathbf{G} = [\mathbf{g}_1, \ldots, \mathbf{g}_K]$ and power allocation vector $\mathbf{p} = [p(1), \ldots, p(K)]^T$. To balance the $SINR_i^{UL}(\mathbf{G}, \mathbf{p})$ among different users, the max-min fairness is adopted in this work as follows

$$\begin{aligned} \underset{\mathbf{G},\mathbf{p}}{\text{maximize}} \quad & \min_j \frac{p(j)}{[\mathbf{D}]_{jj}(\mathbf{\Phi}_j^T\mathbf{p} + \sigma^2)} \\ \text{subject to} \quad & \mathbf{p} \succeq \mathbf{0}, \mathbf{p} \preceq \mathbf{p}_{max}, \|\mathbf{g}_i\|_2 = 1,\ i = 1, \ldots, K, \end{aligned} \quad (4)$$

where $\mathbf{p}_{max}$ denotes the vector of individual maximal transmit power, and $\mathbf{0}$ is an all-zero vector with K elements. In an attempt to maximize the entire network throughput, by using the log utility functions, the proportional fairness criterion pulls up the weaker signals thereby giving them QoS protections. However, the QoS protection from proportional fairness is not as strong as that of the max-min criterion. Because the fairness is the top concern in the multiuser uplinks, rather than the entire throughput, in this work with the purpose to address the strong-weak spatial-temporal resonances the max-min criterion is selected.

By introducing an auxiliary variable γ and rewriting the K individual SINR expressions into a vector form, we have

$$\begin{aligned} \underset{\mathbf{G},\mathbf{p},\gamma}{\text{maximize}} \quad & \gamma \\ \text{subject to} \quad & \mathbf{p} \succeq \mathbf{0}, \mathbf{p} \preceq \mathbf{p}_{max}, \mathbf{p} \succeq \gamma\mathbf{D}(\mathbf{\Phi}^T\mathbf{p} + \boldsymbol{\sigma}), \\ & \|\mathbf{g}_i\|_2 = 1,\ i = 1, \ldots, K, \end{aligned} \quad (5)$$

where $\boldsymbol{\sigma}$ is a $K \times 1$ vector with each element being σ^2.

First of all, the optimization problem in (5) is not convex. Moreover, the $4 \times K$ individual constraints make the problem even more challenging. To solve (5), we develop a two-stage efficient algorithm as will be shown in the following two sections. Specifically, we first relax the problem into a Perron Frobenius eigenvalue optimization problem through using a total power constraint to enlarge the feasible set, and develop an iterative algorithm to find the optimal solution to the relaxed problem. Then, we propose an adaptive two-stage algorithm to find the global optimal solution to the original optimization problem with individual constraints, based on the relaxed eigenvalue problem.

III. Iterative Algorithm with a Total Power Constraint

In this section, we will introduce our work on relaxing the original uplink SINR balancing problem into an equivalent eigenvalue optimization problem and introduce the proposed algorithm where the signature and power assignment are iteratively optimized.

The relaxed version of the original problem in (5) is

$$\begin{aligned} \underset{\mathbf{G},\mathbf{p},\gamma}{\text{maximize}} \quad & \gamma \\ \text{subject to} \quad & \mathbf{1}^T\mathbf{p} \leq \mathbf{1}^T\mathbf{p}_{max}, \mathbf{p} \succeq \gamma\mathbf{D}(\mathbf{\Phi}^T\mathbf{p} + \boldsymbol{\sigma}), \\ & \mathbf{p} \succeq \mathbf{0}, \|\mathbf{g}_i\|_2 = 1,\ i = 1, \ldots, K, \end{aligned} \quad (6)$$

where $\mathbf{1}$ is an all-one vector with K elements.

Here we can see, the problem in (6) maintains the same objective function but is relaxed by a total power constraint.

A. Uplink Power Assignment Problem

We first consider the case when the signature matrix is fixed as $\tilde{\mathbf{G}} = [\tilde{\mathbf{g}}_1, \tilde{\mathbf{g}}_2, \ldots, \tilde{\mathbf{g}}_K]$ with $\|\tilde{\mathbf{g}}_i\|_2 = 1, i = 1, 2, \ldots, K$, and then problem in (6) is reduced to an uplink power allocation problem as

$$\begin{aligned} \underset{\mathbf{p},\gamma}{\text{maximize}} \quad & \gamma \\ \text{subject to} \quad & \mathbf{p} \succeq \mathbf{0}, \mathbf{1}^T\mathbf{p} \leq \mathbf{1}^T\mathbf{p}_{max}, \mathbf{p} \succeq \gamma\mathbf{D}(\mathbf{\Phi}^T\mathbf{p} + \boldsymbol{\sigma}). \end{aligned} \quad (7)$$

In Theorem 1, the necessary condition for the global optimum of problem in (7) is introduced.

Theorem 1: Given $\tilde{\mathbf{G}}$, if $\mathbf{p}^*$ is a global maximizer of the (7), then $\mathbf{1}^T\mathbf{p}^* = \mathbf{1}^T\mathbf{p}_{max}$, and $\mathbf{p}^* = \gamma^*\mathbf{D}(\mathbf{\Phi}^T\mathbf{p}^* + \boldsymbol{\sigma})$, where γ^* is the optimum of minimum weighted SINR.

Proof: The proof of Theorem 1 is in APPENDIX A. ■

Combining the two equations in Theorem 1, we have an equivalent necessary condition for global optimizer $\mathbf{p}^*$ of (7) as $\frac{1}{\gamma^*}\mathbf{1}^T\mathbf{p}_{max} = \mathbf{1}^T\mathbf{D}(\mathbf{\Phi}^T\mathbf{p}^* + \boldsymbol{\sigma})$.

Based on the previous analysis, let us define an augmented power vector as $\tilde{\mathbf{p}} = [\mathbf{p}^T, 1]^T$ and an augmented matrix which only depends on $\mathbf{G}$ and $P_{total} = \mathbf{1}^T\mathbf{p}_{max}$ as

$$\mathbf{\Lambda}(\mathbf{G}, P_{total}) = \begin{pmatrix} \boldsymbol{D\Phi^T} & \boldsymbol{D\sigma} \\ \frac{1}{P_{total}}\mathbf{1}^T\boldsymbol{D\Phi^T} & \frac{1}{P_{total}}\mathbf{1}^T\boldsymbol{D\sigma} \end{pmatrix}. \quad (8)$$

Then, the necessary condition for the global optimum $\mathbf{p}^*$ in (7) can be characterized as an eigensystem that $\frac{1}{\gamma^*}\tilde{\mathbf{p}}^* = \Lambda(\mathbf{G}, P_{total})\tilde{\mathbf{p}}^*$. In order to ensure the feasibility of the solution, $\tilde{\mathbf{p}}^*$ should be element-wisely positive as well as γ^*.

In TRDMA uplink systems, due to the existence of ISI and IUI, $\mathbf{\Phi}$ is a nonnegative irreducible cross-talk matrix. As a result, $\mathbf{\Lambda}(\mathbf{G}, P_{total})$ is a matrix with nonnegative entries and is also irreducible. According to the Perron Frobenius Theorem [27], [34], [35], we can have the following properties for $\mathbf{\Lambda}$ as

1) the maximal eigenvalue λ_{max} is just its spectral radius and it is simple;
2) the eigenvector $\mathbf{v}$ that has all positive entries is the one associated to the largest eigenvalue.

Therefore, there exists a feasible solution to the eigensystem and the solution is unique. Moreover, based upon the uniqueness and existence, the necessary condition in Theorem 1 becomes a necessary and sufficient condition for global optimum of (7). Thus, the power allocation problem in (7) is addressed by finding the Perron Frobenius eigenvector of $\mathbf{\Lambda}(\tilde{\mathbf{G}}, P_{total})$ and the optimal threshold is given by $\gamma^* = 1/\lambda_{max}(\mathbf{\Lambda}(\tilde{\mathbf{G}}, P_{total}))$.

B. Joint Signature Design and Power Assignment

From the previous subsection, we know that for any arbitrary matrix $\tilde{\mathbf{G}}$, the optimal power assignment vector $\mathbf{p}^*$ under the total power constraint P_{total} is a $K \times 1$ vector consisting of the first K elements in the scaled $(K+1) \times 1$ dominant eigenvector of $\mathbf{\Lambda}(\tilde{\mathbf{G}}, P_{total})$. Meanwhile the associated optimal threshold γ^* is the reciprocal of the dominant eigenvalue. Therefore, the number of optimization variables in (6) is greatly reduced and the (6) is equivalent to an eigenvalue optimization problem as

$$\begin{aligned} &\underset{\mathbf{G}}{\text{minimize}} \quad \lambda_{max}(\mathbf{\Lambda}(\mathbf{G}, P_{total})) \\ &\text{subject to} \quad \|\mathbf{g}_i\|_2 = 1, \ i = 1, \ldots, K, \end{aligned} \tag{9}$$

For the Perron Frobenius eigenvalue λ of a matrix $\mathbf{\Lambda}$, it can be represented as [35]

$$\lambda = \min_{\mathbf{y} \succ 0} \max_{\mathbf{x} \succ 0} \frac{\mathbf{x}^T \mathbf{\Lambda} \mathbf{y}}{\mathbf{x}^T \mathbf{y}} = \min_{\mathbf{x} \succ 0} \max_{\mathbf{y} \succ 0} \frac{\mathbf{x}^T \mathbf{\Lambda} \mathbf{y}}{\mathbf{x}^T \mathbf{y}}. \tag{10}$$

Recall that $\tilde{\mathbf{p}} = [\mathbf{p}^T, 1]^T$, let us define a cost function as $\tilde{\lambda}(\mathbf{G}, \mathbf{p}) = \max_{\mathbf{x} \succ 0} \mathbf{x}^T \mathbf{\Lambda}(\mathbf{G}, P_{total}) \tilde{\mathbf{p}} / \mathbf{x}^T \tilde{\mathbf{p}}$, and the Perron Frobenius eigenvalue can be represented as $\lambda_{max}(\mathbf{\Lambda}(\mathbf{G}, P_{total})) = \min_{\mathbf{p} \succ 0} \tilde{\lambda}(\mathbf{G}, \mathbf{p})$.

Then, the optimal threshold for the problem in (9) can be obtained as

$$\gamma^* = \frac{1}{\min_{\mathbf{G}} \min_{\mathbf{p} \succ 0} \tilde{\lambda}(\mathbf{G}, \mathbf{p})} = \frac{1}{\min_{\mathbf{G}} \tilde{\lambda}(\mathbf{G}, \mathbf{p}_{opt})}, \tag{11}$$

where $\mathbf{p}_{opt} = \arg \min_{\mathbf{p} \succ 0} \tilde{\lambda}(\mathbf{G}, \mathbf{p})$ represents a vector consisting of the first K elements in the dominant eigenvector.

Given the cost function, the problem in (9) has an equivalent formulation as

$$\min_{\mathbf{G}} \min_{\mathbf{p} \succ 0} \tilde{\lambda}(\mathbf{G}, \mathbf{p}) \Leftrightarrow \min_{\mathbf{p} \succ 0} \min_{\mathbf{G}} \tilde{\lambda}(\mathbf{G}, \mathbf{p}). \tag{12}$$

For the left part in (12), when the signature matrix is fixed, the problem is solved as the eigenvalue problem in the previous subsection. Considering the right hand side of (12), when the power allocation vector is fixed, the way to find the corresponding optimal signature matrix $\mathbf{G}^*$ is given in Lemma 1 as follows.

Lemma 1: The optimal signature matrix for a given vector $\mathbf{p}_{ary}$ is denoted as $\mathbf{G}^*$. We have $\mathbf{G}^* = \arg \min_{\mathbf{G}} \tilde{\lambda}(\mathbf{G}, \mathbf{p}_{ary}) = \arg \min_{\mathbf{G}} \gamma_i / SINR_i^{UL}(\mathbf{G}, \mathbf{p}_{ary}), \forall i$. That is to say, the optimal signature can be obtained by individually maximizing the uplink SINR of each user.

Proof: The proof of Lemma 1 is in APPENDIX B. ■

Algorithm 1. Iterative SINR Balancing Algorithm under Total Power Constraint

1: **Initialize:** Given $\{\gamma_i\}_{i=1}^K$, σ^2, $\mathbf{R}_i$ and $\mathbf{R}_i^{(0)}$ $\forall i$, $\mathbf{P}_{max}$. Pick $\epsilon > 0$, $P_{total} \leftarrow \mathbf{1}^T \mathbf{P}_{max}$, $\mathbf{p}^{(0)} \leftarrow \frac{P_{total}}{K}\mathbf{1}$, $\lambda_{max}^{(0)} \leftarrow \infty$.
2: **loop** $n \Leftarrow n+1$
3: Calculate the MMSE $\mathbf{g}_i^{(n)}, \forall i$ under $\mathbf{p}^{(n-1)}$, and normalize it to make $\|\mathbf{g}_i\|_2 = 1, \forall i$.
4: Build the couple matrix $\mathbf{\Lambda}^{(n)}(\mathbf{G}^{(n)}, P_{total})$ in the way shown in (8).
5: Solve the Perron Frobenius eigenpair problem to get $\lambda_{max}^{(n)}$ and its corresponding eigenvector $\tilde{\mathbf{p}}^{(n)}$ with $\tilde{p}^{(n)}(K+1) = 1$. $\mathbf{p}^{(n)} \leftarrow \{\tilde{\mathbf{p}}^{(n)}\}_1^K$.
6: **end loop** If $\lambda_{max}^{(n-1)} - \lambda_{max}^{(n)} < \epsilon$ or reach the maximal number of iterations.

Remark: The SINR maximizing signature can be optimized by

$$\mathbf{g}_i^* = \arg \max_{\|\mathbf{g}_i\|_2 = 1} p_{ary}(i) / [\mathbf{D}]_{ii} (\mathbf{\Phi}_i^T \mathbf{p}_{ary} + \sigma^2), \forall i. \tag{13}$$

The optimal solution is equivalent to the MMSE beamforming vector, $\mathbf{g}_i^* = \alpha_i (\sum_{j=1}^K p_{ary}(j) \mathbf{R}_j + \sigma^2 \mathbf{I})^{-1} \mathbf{H}_i^{(L)H}, \forall i$, where α_i is a normalized factor.

Furthermore, the necessary and sufficient condition for the global optimum of problem in (9) is stated in the following theorem.

Theorem 2: (Necessary and Sufficient Condition): $\mathbf{G}^* = [\mathbf{g}_1^*, \mathbf{g}_2^*, \ldots, \mathbf{g}_K^*]$ is the global optimizer of the problem in (9) if and only if $\tilde{\lambda}(\mathbf{G}^*, \mathbf{p}^*) = \min_{\mathbf{G}} \tilde{\lambda}(\mathbf{G}, \mathbf{p}^*)$, where $\mathbf{p}^* = \arg \min_{\mathbf{p} \succ 0} \tilde{\lambda}(\mathbf{G}^*, \mathbf{p})$, i.e., $\tilde{\mathbf{p}}^*$ is the Perron Frobenius eigenvector of $\mathbf{\Lambda}(\mathbf{G}^*, P_{total})$ and $\tilde{\mathbf{p}}^{*T} = [\mathbf{p}^{*T}, 1]$.

Proof: The proof of Theorem 2 is in APPENDIX C. ■

Theorem 2 implies that if one of the variable $\mathbf{p}$ or $\mathbf{G}$ has reached the optimum, the remaining one can be obtained either by solving the Perron Frobenius eigenpair problem or by independently solving the MMSE problem. Based on this, we propose an iterative algorithm that alternatively optimizes $\mathbf{p}$ and $\mathbf{G}$, and eventually converges to the global optimum.

C. Iterative Algorithm and Convergence

Built upon the previous analysis, we propose an iterative algorithm in Algorithm 1 to jointly optimize the signature matrix and the power assignment vector, given the objective to balance the weighted uplink SINRs for all users.

Theorem 3: The sequence $\{\lambda_{max}^{(n)}\}_{n=0}^{\infty}$ generated by the proposed algorithm in Algorithm 1 is strictly decreasing and converges to the global optimum of (9), regardless of the initial value.

Proof: The proof of Theorem 3 is in APPENDIX D. ■

As we proved, the necessary and sufficient condition for global optimum of (9) is equivalent to the condition $\lambda_{max}^{(n+1)} = \lambda_{max}^{(n)}$, which implies the convergence of $\{\lambda_{max}^{(n)}\}$ sequence. As a consequence, the algorithm stops as soon as the difference in $\lambda_{max}^{(n-1)} - \lambda_{max}^{(n)}$ reaches a predetermined threshold $\epsilon > 0$. On

average the algorithm will yield the global optimum of (9) in 3 or 4 iterations, independent of number of users.

IV. Two-Stage Adaptive Algorithm With Individual Power Constraints

In the previous section, we have discussed how to relax the original problem in (5) into a Perron Frobenius eigenvalue optimization problem. For any fixed total power constraint P_{total}, there only exists one pair of optimal signature matrix $\mathbf{G}^*(P_{total})$ and power assignment vector $\mathbf{p}^*(P_{total})$. As we have analyzed, the original problem with individual power constraints has a more tightened feasible set. Hence, we need to gradually shrink the relaxed feasible set until the optimal solution to the original problem is reached.

Lemma 2: The optimal power assignment vector generated from iterative SINR balancing algorithm in Algorithm 1 is monotonically increasing as the total power constraint P_{total} increases.

Proof: The proof is provided in APPENDIX E. ■

According to Lemma 2, we know that as the feasible set is shrunk by reducing the total power constraint in (6), the optimal power assignment for each user is monotonically decreasing. Hence, as long as we keep adjusting the feasible set by updating the total power constraint, we will definitely reach a point which is on the boundary of the individual-constrained feasible set. At this point, we achieve the maximum of balanced weighted SINRs. In the SINR balancing scenario under TRDMA uplink systems, the user with the weakest spatial-temporal resonance or a minimal transmit power will restrict the performance of entire system. Here, we define the worst case in a network to be the user who has a minimal difference between its power constraint $p_{max}(i)$ and its assigned power under a total power constraint P_{total}, i.e. $p_{max}(i) - p_i^*(P_{total})$. After finding the worst case, the relaxed feasible set is updated following the direction of the worst case.

The proposed two-stage adaptive algorithm is shown in Algorithm 2, where the SINR balancing problem with individual constraints is solved. In stage I, the original optimization problem in (5) is relaxed into an eigenvalue optimization problem, and the corresponding optimum is obtained through the proposed iterative algorithm shown in Algorithm 1. In stage II, based on the solution in stage I, the relaxed feasible set is modified by updating the total power constraint using the gradient decent method against the worst case. Before converging to the global optimum, stage I and stage II work alternatively and iteratively.

A. Analysis on Convergence

Theorem 4: The sequence $\{\delta^{(n)}, n = 1, 2, \ldots\}$ generated from Algorithm 2, is a strictly increasing sequence, and converges to 0 where the global optimum for problem in (5) is achieved.

Proof: The proof is provided in APPENDIX F. ■

According to Theorem 4, we can see that our adaptive algorithm for SINR balancing problem under individual power constraints is practical and it always converges to the global optimal solution to the problem in (5).

Algorithm 2. Two-Stage Adaptive Algorithm for SINR Balancing Problem under Individual Power Constraint

1: **Initialize:** Given $\{\gamma_i\}_{i=1}^K$, σ^2, $\mathbf{R}_i$ and $\mathbf{R}_i^{(0)}$ $\forall i$, $\mathbf{P}_{max}$. Pick $\epsilon > 0$ as the stop criterion or tolerance and $0 < \eta, \mu < 1$ as stepsizes. $P_{total}^{(0)} \leftarrow \mathbf{1}^T\mathbf{P}_{max}$, Update $\mathbf{p}^{(0)}$ by Algorithm 1 under $P_{total}^{(0)}$, $\delta\mathbf{p}^{(n)} \leftarrow \mathbf{P}_{max} - \mathbf{p}^{(n)}$, [index, $\delta^{(n)}$] $\leftarrow \min(\delta\mathbf{p}^{(n)})$.
2: **loop** $n \Leftarrow n + 1$
3: $\mathbf{p} \leftarrow$ Algorithm 1 with $\mu P_{total}^{(n-1)}$, slope $\leftarrow (p^{(n-1)}(\text{index}) - p(\text{index}))/(1-\mu)P_{total}$.
4: $\delta P_{total} \leftarrow \delta^{(n-1)}/\text{slope}$, $P_{total}^{(n)} \leftarrow P_{total}^{(n-1)} + \delta P_{total}$.
5: Update $\mathbf{p}^{(n)}$ under $P_{total}^{(n)}$, $\delta\mathbf{p}^{(n)}$, and [index, $\delta^{(n)}$] $\leftarrow \min(\delta\mathbf{p}^{(n)})$ ▷ Find the worst case
6: **while** $\delta^{(n)} > \epsilon$ **do** ▷ Force $\delta^{(n)} \le \epsilon$
7: $\delta P_{total} \leftarrow \eta \times \delta P_{total}$, $P_{total}^{(n)} \leftarrow P_{total}^{(n-1)} + \delta P_{total}$
8: Update $\mathbf{p}^{(n)}$, $\delta\mathbf{p}^{(n)}$ and [index, $\delta^{(n)}$]
9: **end while**
10: **end loop** If $|\delta^{(n)}| \le \epsilon$ or reach the maximal number of iterations.

The average number of iterations for Algorithm 1 to converge is $N_1 = 3$, for backward search in Algorithm 2 with stepsize $\eta = 0.8$ is $N_2 = 1$, and for Algorithm 2 with stepsize $\mu = 0.9$ is $N_3 = 3$. Moreover, the complexity for solving MMSE signature is $O(L^2)$, where L is the length of channel. In our real environment measurement, under 125 MHz its typical value is smaller than 30. The computational complexity for solving the Perron Frobenius eigenvalue of the augmented matrix is $O((K+1)^2)$, where K is the number of users in the uplinks. Hence, the total computational complexity for the joint optimization is approximately $N_1 \times N_2 \times (1 + N_3) \times (O(L^2) + O((K+1)^2))$. Under the simulation with stepsizes being $\eta = 0.8$ and $\mu = 0.9$, the amount of required computation time is $10 \times (O(L^2) + O((K+1)^2))$.

B. Properties of SINR Balancing Problem

In this part, we will briefly introduce some properties of the TRDMA SINR balancing problem.

Assumption 1: With a small perturbation in total power constraint P_{total}, i.e., $P_{total} \to (1+\Delta)P_{total}$, $\Delta \ll 1$, the optimal MMSE signature can be viewed as approximately unchanging.

The detailed explanation for the rationality of Assumption 1 is shown in APPENDIX G.

Following the Assumption 1, as $\Delta < 10^{-2}$, since the optimal MMSE signature matrix $\mathbf{G}$ will not change, the argumented matrix $\mathbf{\Lambda}(\mathbf{G}, P_{total})$ in (8) will have the same components with $\mathbf{\Lambda}(\mathbf{G}, (1+\Delta)P_{total})$ except the last row. Under this setting, we have

$$\mathbf{\Lambda}(\mathbf{G}, (1+\Delta)P_{total}) = \begin{pmatrix} \boldsymbol{D\Phi^T} & \boldsymbol{D\sigma} \\ \frac{\mathbf{1}^T\boldsymbol{D\Phi^T}}{(1+\Delta)P_{total}} & \frac{\mathbf{1}^T\boldsymbol{D\sigma}}{(1+\Delta)P_{total}} \end{pmatrix}, \quad (14)$$

and $\mathbf{\Lambda}(\mathbf{G}, (1+\Delta)P_{total}) = \mathbf{A} \times \mathbf{\Lambda}(\mathbf{G}, P_{total})$, where $\mathbf{A} = \begin{pmatrix} \mathbf{I} & \mathbf{0} \\ \mathbf{0}^T & \frac{1}{1+\Delta} \end{pmatrix}$.

As mentioned in [39], $\rho(\mathbf{\Lambda}(\mathbf{G}, (1+\Delta)P_{total})) \geq \frac{1}{(1+\Delta)^{\alpha}}\rho(\mathbf{\Lambda}(\mathbf{G}, P_{total}))$ and $\delta\lambda \geq (\frac{1}{(1+\Delta)^{\alpha}} - 1)\lambda$, where $\delta\lambda$ is the difference in dominant eigenvalues, $\rho(\cdot)$ denotes the spectral radius of nonnegative matrices, i.e., in our case it is the Perron Frobenius eigenvalue, and $0 < \alpha < 1$ is a coefficient determined by the right and left Perron Frobenius eigenvectors of $\mathbf{\Lambda}(\mathbf{G}, P_{total})$.

Then, we can bound the change of Perron Frobenius eigenvalue under the perturbation of Δ as $0 < -\frac{\delta\lambda}{\lambda} < \frac{\Delta}{\Delta+1}$.

Let us denote $\mathbf{k} = [k_1, k_2, \ldots, k_K]$ as the optimal power assignment ratio vector, where $k_i = p^*(i)/P_{total}$ and $p^*(i)$ is the optimal power assignment to problem in (6) under total power constraint P_{total}. According to the necessary and sufficient condition of optimal power, we have

$$\mathbf{k} = \frac{1}{P_{total}}(\lambda\mathbf{I} - \mathbf{D}\mathbf{\Phi}^T)^{-1}\mathbf{D}\mathbf{1}, \tag{15}$$

where we assume $\boldsymbol{\sigma} = \mathbf{1}$ and thus P_{total} is the SNR. Then we can also have

$$\begin{aligned}\mathbf{k} + \delta\mathbf{k} &= \frac{1}{(1+\Delta)P_{total}}((\lambda+\delta\lambda)\mathbf{I} - \mathbf{D}\mathbf{\Phi}^T)^{-1}\mathbf{D}\mathbf{1} \\ &= \frac{1}{1+\Delta}\sum_{n\geq 0}\left(-\frac{\delta\lambda}{\lambda}\left(\mathbf{I} - \frac{1}{\lambda}\mathbf{D}\mathbf{\Phi}^T\right)^{-1}\right)^n \mathbf{k}, \end{aligned} \tag{16}$$

where $\delta\mathbf{k}$ denotes the change in power assignment ratio with a total power changes by ΔP_{total}.

Combining the (15) and the (16), we can represent the change in power assignment ratio vector as $\delta\mathbf{k} = -\frac{\Delta}{1+\Delta}\mathbf{k} + \frac{1}{1+\Delta}\sum_{n\geq 1}(-\frac{\delta\lambda}{\lambda}\mathbf{C}^{-1})^n\mathbf{k}$, where $\mathbf{C}^{-1} = (\mathbf{I} - \frac{1}{\lambda}\mathbf{D}\mathbf{\Phi}^T)^{-1}$, and $\sum_{n\geq 1}(-\frac{\delta\lambda}{\lambda}\mathbf{C}^{-1})^n$ exists. It can be further derived as

$$\begin{aligned}\delta\mathbf{k} &= \frac{\Delta}{1+\Delta}\left(-\mathbf{I} + \frac{1}{\Delta}\sum_{n\geq 1}\left(-\frac{\delta\lambda}{\lambda}\mathbf{C}^{-1}\right)^n\right)\mathbf{k} \\ &= \frac{\Delta}{1+\Delta}\left(\mathbf{I} + \frac{\delta\lambda}{\lambda}\mathbf{C}^{-1}\right)^{-1}\left(-\frac{\Delta+1}{\Delta}\frac{\delta\lambda}{\lambda}\mathbf{C}^{-1} - \mathbf{I}\right)\mathbf{k}. \end{aligned} \tag{17}$$

Moreover, owing to the fact that $\mathbf{1}^T\delta\mathbf{k} = 0$, $\mathbf{1}^T\mathbf{k} = 1$, we have $1 = \mathbf{1}^T(-\frac{\Delta+1}{\Delta}\frac{\delta\lambda}{\lambda}\mathbf{C}^{-1})\mathbf{k}$.

Let us define $\mathbf{v} = -\frac{\Delta+1}{\Delta}\frac{\delta\lambda}{\lambda}\mathbf{C}^{-1}\mathbf{k}$, with $0 < v_i, \ \forall i < 1$ and $\mathbf{1}^T\mathbf{v} = 1$. The (17) can be re-written as $\delta\mathbf{k} = \frac{\Delta}{1+\Delta}(\mathbf{I} + \frac{\delta\lambda}{\lambda}\mathbf{C}^{-1})^{-1}(\mathbf{v} - \mathbf{k})$. Dividing both sides by Δ, we have $\frac{\delta\mathbf{k}}{\Delta} = \frac{1}{1+\Delta}(\mathbf{I} + \frac{\delta\lambda}{\lambda}\mathbf{C}^{-1})^{-1}(\mathbf{v} - \mathbf{k})$.

Then taking the limit gives $\lim_{\Delta\to 0}\frac{\delta\mathbf{k}}{\Delta} = (\mathbf{v} - \mathbf{k})$, which implies that $\lim_{\delta P\to 0}\frac{\delta k_i}{\delta P} = \frac{1}{P_{total}}(v_i - k_i), \forall i$, where δP is the perturbation in P_{total}. This demonstrates that the slope $\frac{|\delta k_i|}{\delta P}$ for every user is bounded by $\frac{1}{P_{total}}\max\{k_i, 1-k_i\}$. As a result, within a suitable SNR range where the slope $\frac{|\delta k_i|}{\delta P}$ is quite small, the optimal power assignment ratio will stay stable even the total power constraint is changing.

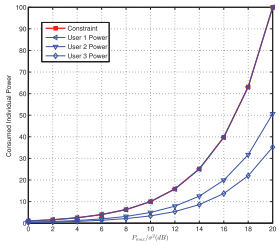

Fig. 3. Power assignment under 3 users case.

V. Simulation Results

To evaluate the proposed algorithms, we conduct several simulations to demonstrate that our proposed weighted SINR balancing algorithm is an ideal solution to ensure fairness and energy-efficiency, as well as to tackle the strong-weak spatial-temporal resonances in the multiuser TRDMA uplink system.

Our simulation settings are described as following:

1) Channel Model: UWB office non-line-of-sight channel, with bandwidth $B = 500$ MHz and maximal number of channel taps $L = 60$.
2) Back-off rate D: The D is set to 4 (16) when there are 3 (20) users.
3) Channel Gain $\|\mathbf{H}_i^{(L)}\|_2^2$: uniform distributed among [0, 1] for all users.
4) Weighted factors: $\gamma_i = 1, \forall i$. Equal maximal power constraint $p_{max}(i) = p_{max}, \forall i$.

A. Optimal Power Assignment

In Fig. 3, we show the optimal power assignment strategy versus the maximal individual power constraint. In this simulation, the channel gains for all 3 users are predetermined as $\|\mathbf{H}_1^{(L)}\|_2^2 : \|\mathbf{H}_2^{(L)}\|_2^2 : \|\mathbf{H}_3^{(L)}\|_2^2 = 1:2:3$, i.e., the 1^{st} user has the worst channel response and may suffer the strong-weak spatial-temporal resonances. Under the equal power constraint setting, in order to balance the weighted SINRs, the worst user always uses up all power to boost SINR while others slightly reduce their transmit power to alleviate interference. Meanwhile, the 3^{rd} user takes an advantage of its focusing effect such that only smallest power is consumed to maintain the balanced SINR. Moreover, the power assignment ratio between all users is approximately stable when the individual power constraint changes.

B. Comparison under Different Backoff Rates

In Fig. 4, 5 and 6, the performance of our proposed algorithm under different backoff rates is studied. For a smaller D, the uplink transmission is conducted more frequently which causes the ISI to lie close to the signal peak at the receiver side. On the other hand, IUI and ISI can be significantly alleviated by choosing a higher backoff rate D. As BER is a monotonically decreasing function in uplink SINR, users' BER in our scheme is also reducing when the backoff rate increases as shown in Fig. 4. In Fig. 5, the balanced SINR becomes higher as the backoff rate increases.

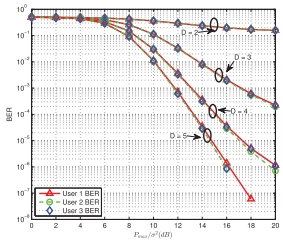

Fig. 4. BER performance comparison under different backoff rates and 3 users.

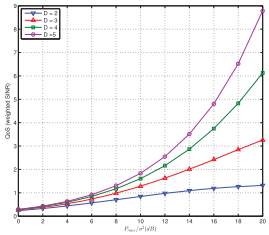

Fig. 5. Balanced SINR comparison under different backoff rates and 3 users.

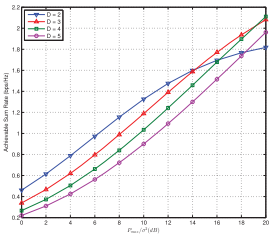

Fig. 6. Achievable sum rate comparison under different backoff rates and 3 users.

Let us define the achivable sum rate in TR uplinks as $\frac{1}{D}\sum_{i=1}^{K}\log_2(1+SINR_i^{UL})$ bps/Hz. Because the achievable sum rate is normalized by $1/D$, a higher D may result in a larger factor in the denominator outside the logarithm which leads to a smaller sum rate. From Fig. 6 we can see that, in low SNR region, a smaller D will always attain a higher sum rate. It is because when the SNR is small, the dominant interference at the receiver side is noise while ISI is less prominnet in the normalized sum rate. On the other hand, as SNR increases, the ISI and IUI become dominant against the noise. Thus, a higher D will reduce those interference efficiently and provide a better sum rate performance.

C. Highly Crowded Network

We then compare the multiuser uplink performance of our proposed algorithm and other two schemes: Basic TR and MMSE TR. In Basic TR scheme, each user transmits with its maximal power and the signature filter $\mathbf{g}_i$ is the normalized time-reversal conjugate version of its channel response,

$$g_i[k]=\frac{h_i^*[L-1-k]}{\sqrt{\sum_{l=0}^{L-1}|h_i[l]|^2}},\quad k=0,\ 1,\ 2,\ \ldots,\ L-1. \quad (18)$$

In MMSE TR, each user also transmits in the maximal power but its signature $\mathbf{g}$ is the MMSE signature that can be calculated by independently maximizing its own SINR.

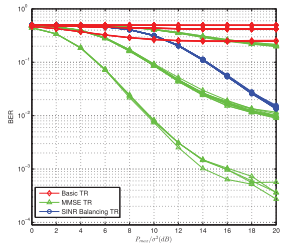

Fig. 7. BER performance comparison under 20 users case.

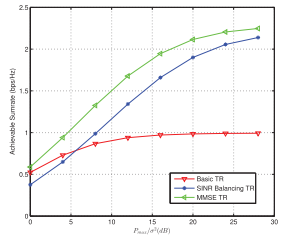

Fig. 8. Achievable sum rate comparison under 20 users case.

On the other hand, in our SINR balancing scheme, AP which has all channel information controls the transmit power of each user and designs the signature filter based on the optimal power assignment.

In this part, we simulate a highly crowded network where one AP serves 20 users. We assume the 20 users are divided into 3 groups according to the strength of their spatial-temporal resonances. The channel gain of each user is set to be $\frac{1}{3}$, $\frac{2}{3}$ or 1, and the back-off rate is $D=16$. Simulations are conducted to compare the BER performance, achievable sum rate, network-level energy-efficiency and user-level energy-efficiency among Basic TR scheme, MMSE TR scheme and the proposed scheme.

In Fig. 7, we can see the BER performances of the aforementioned three schemes in a highly crowded network. All users in Basic TR scheme have such a high BER that the whole system fails to work properly. With MMSE TR, some of users whose channel degradation is severe will have a poor BER performance that is close to the Basic TR BER curves. Thus, even when they are active and transmitting in full power, those users are blocked from getting service due to the low SINRs. Moreover, these blocked users bring high interference to other active users which degrades the whole network's performance. On the other hand, when applying our proposed algorithm to this crowded network, as SINRs are balanced, all users will have almost the same rational BER performance such that all of them can be detected. This indicates that the proposed algorithm can support all users, no matter whether their spatial-temporal resonance is strong or weak and no matter how crowded the network is.

Fig. 8 shows the curves of achievable sum rate versus the maximal power constraint. Here, the achievable sum rate is normalized by $1/D$ which represents the spectral efficiency. Since Basic TR is aimed to maximize the received signal power regardless of interference, it saturates at a lower rate. In this case, because the interference of other users becomes the dominant factor in individual SINRs and the channels become more correlated as the number of users is large, even under maximal power Basic TR fails to support the system with a high quality

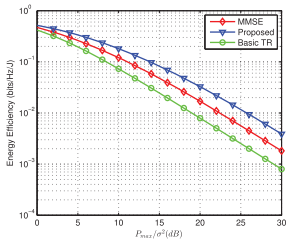

Fig. 9. Network-level energy-efficiency comparison under 20 users case.

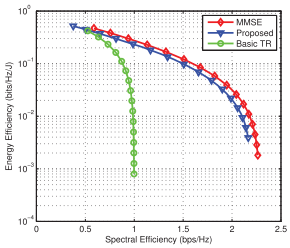

Fig. 10. Trade-off between energy-efficiency and spectral-efficiency under 20 users case.

of service. In MMSE TR scenario, as everyone transmits in maximal power and MMSE signature is applied at AP to extract information, the SINR is boosted remarkably. As a result, even the network is highly densed and the interference is large, MMSE signature can surpress the interference and the MMSE TR obtains a higher achievable rate than Basic TR. In SNR balancing scheme, users with a better spatial-temporal resonance has to sacrifice to achieve the balance, leading to a reduction in the sum rate compared to the MMSE TR. However, the gap between the sum rate of MMSE TR and proposed scheme diminishes in high SNR range.

The energy-efficiency feature of our proposed scenario is further studied in Fig. 9, Fig. 10 and Fig. 11. In Fig 9, the network-level energy-efficiencies of different schemes are plotted versus the individual power constraints. Here, we define the network-level energy-efficiency as the ratio between achievable sum rate and the total transmit power: Energy-Efficiency (bits/Hz/J) $= \frac{\text{Achievable sum rate (bps/Hz)}}{\text{Total power consumed in the network (W)}}$. Under the same condition, the network-level energy-efficiency of the proposed scheme is higher than those of the MMSE TR and the Basic TR. That is because in the MMSE TR and Basic TR, most of the energies are wasted to generate interference, and thus the network performance are contaminated. In the proposed algorithm, by the means of joint signature matrix and power allocation optimization, the interference between users are well managed and resources are assigned efficiently.

The trade-off between energy-efficiency and spectral-efficiency is shown in Fig 10. As we can see, for a given spectral-efficiency, the energy-efficiency of the proposed algorithm is lower than that of the MMSE TR. The reason is that since the proposed algorithm is aimed to balance the weighted uplink SINRs which is restricted by the worst users, the power consumption to achieve the same total network throughput is higher. However, this does not contradict with the result in Fig 9, since in order to have a fair comparison we must fix the individual power constraints for all the different schemes to be the same. As we have shown, under the same power constraints,

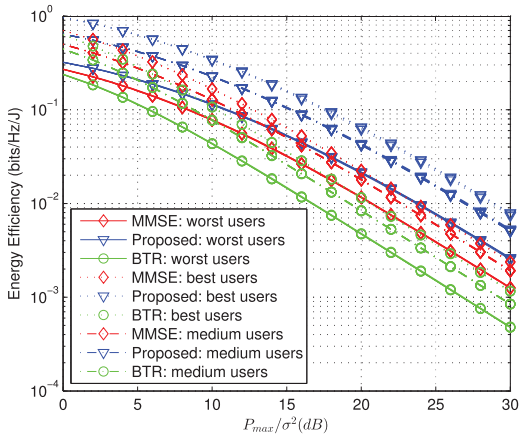

Fig. 11. User-level energy-efficiency comparison under 20 users case.

the proposed algorithm achieves a higher network-level energy-efficiency than others.

Moreover, the user-level energy-efficiency defined as the ratio of per-user throughput to power consumption of the user is studied. As we can see in Fig 11, under the same individual power constraints, the user-level energy-efficiency obtained by the proposed algorithm is superior to those of MMSE TR and Basic TR, for all users. In the proposed scheme, with joint signature design and power allocation, the interference between users is well managed and resource is utilized efficiently with a guarantee on QoS fairness.

Hence, due to the high user-level energy-efficiency, no matter how strong their spatial-temporal resonances are, each users have an incentive and prefer the proposed algorithm to the others.

As demonstrated in Fig 9 and 11, under the same power constraints, both the network-level energy-efficiency and user-level energy-efficiency are improved remarkably through our proposed algorithm, compared with MMSE TR and Basic TR. The reason is that by the means of joint signature design and power allocation optimization, the severe interference between users is alleviated and weak spatial-temporal resonance is also compensated. Moreover, the purpose of our proposed algorithm is to balance the weighted uplink SINRs among all users. When equal weighted factors are adopted, the proposed algorithm achieves a same uplink SINR for all users, providing a fair QoS guarantee. On the other hand, heterogenous QoS requirements can be achieved by selecting different weighted factors. Hence, the proposed algorithm is energy-efficient and QoS-guaranteed in multiuser TRDMA uplinks.

VI. Conclusion

In this paper, we propose a joint power allocation and signature design method to address the strong-weak spatial-temporal resonances in multiuser TRDMA uplink systems. By forming the TRDMA strong-weak spatial-temporal resonances problem into a max-min weighted SINR problem, a two-stage adaptive algorithm that can guarantee to converge to the global optimal solution is proposed. In stage I, the original non-convex optimization problem is relaxed into a Perron Frobenius eigenvalue optimization problem whose optimum can be efficiently

obtained. In stage II, the gradient descent method is applied to adaptively update the relaxed feasible set until the prime global optimum that satisfies all individual constraints is reached. In our simulation, the proposed algorithm converges to the global optimum in a few iterations with a relatively low computational complexity. Moreover, the proposed algorithm provides a high energy-efficiency and a QoS performance guarantee to all users in network. Simulation results also show that, our method is capable of boosting the entire system performance through signature design and power allocation. Therefore, the proposed SINR balancing algorithm can be a promising technique for energy-efficient QoS-guaranteed multiuser TRDMA uplink systems.

APPENDIX A
PROOF OF THEOREM 1

Proof: For the problem in (7), suppose a global optimizer $\hat{\mathbf{p}}$ is obtained, and $\hat{\gamma}$ is the achievable maximal threshold within the feasible set. For some index n_0, we have $\hat{p}(i)/[\mathbf{D}]_{ii}(\mathbf{\Phi}_i^T\hat{\mathbf{p}}+\sigma^2)=\hat{\gamma},\ i=n_0$, and $\hat{p}(i)/[\mathbf{D}]_{ii}(\mathbf{\Phi}_i^T\hat{\mathbf{p}}+\sigma^2)\geq\hat{\gamma},\ \forall i\neq n_0$.

First of all, suppose $\mathbf{1}^T\hat{\mathbf{p}}<\mathbf{1}^T\mathbf{p}_{max}$, i.e., there is a portion of unused energy at the optimum point as $P_{save}=\mathbf{1}^T\mathbf{p}_{max}-\mathbf{1}^T\hat{\mathbf{p}}$. If we re-distribute P_{save} among all the users such that the updated power assignment vector is $\hat{\mathbf{p}}_{new}=\alpha\hat{\mathbf{p}}$ with $\alpha>1$ and $\mathbf{1}^T\hat{\mathbf{p}}_{new}=\mathbf{1}^T\mathbf{p}_{max}$. Obviously, $\hat{\mathbf{p}}_{new}$ is in the feasible set defined in (7). Thus, we get $\frac{\hat{p}_{new}(i)}{[\mathbf{D}]_{ii}(\mathbf{\Phi}_i^T\hat{\mathbf{p}}_{new}+\sigma^2)}=\frac{\hat{p}(i)}{[\mathbf{D}]_{ii}(\mathbf{\Phi}_i^T\hat{\mathbf{p}}+\frac{\sigma^2}{\alpha})}\geq\hat{\gamma}_{new}>\hat{\gamma}$, which contradicts to the assumption that $\hat{\gamma}$ is the maximum within the feasible set. Hence, when the global optimum γ^* is achieved, we must have $\mathbf{1}^T\mathbf{p}^*=\mathbf{1}^T\mathbf{p}_{max}$, and the optimal threshold γ^* is a monotonically increasing function in $P_{total}=\mathbf{1}^T\mathbf{p}_{max}$.

Suppose when γ^* is achieved with the optimal power assignment vector $\mathbf{p}_1$, for some index n_1, we have $\frac{p_1(n_1)}{[\mathbf{D}]_{n_1n_1}(\mathbf{\Phi}_{n_1}^T\mathbf{p}_1+\sigma^2)}>\gamma^*$, and for other users we have $\frac{p_1(i)}{[\mathbf{D}]_{ii}(\mathbf{\Phi}_i^T\mathbf{p}_1+\sigma^2)}=\gamma^*,\ \forall i\neq n_1$. Moreover, $\frac{p(i)}{[\mathbf{D}]_{ii}(\mathbf{\Phi}_i^T\mathbf{p}+\sigma^2)}$ is strictly increasing in $p(i)$ and decreasing in $p(j),\ j\neq i$, since $\partial\frac{p(i)}{[\mathbf{D}]_{ii}(\mathbf{\Phi}_i^T\mathbf{p}+\sigma^2)}/\partial p(i)=\frac{[\mathbf{D}]_{ii}\sum_{j\neq i}\mathbf{\Phi}_{ji}p(j)+\sigma^2}{([\mathbf{D}]_{ii}(\mathbf{\Phi}_i^T\mathbf{p}+\sigma^2))^2}>0$ and $\partial\frac{p(i)}{[\mathbf{D}]_{ii}(\mathbf{\Phi}_i^T\mathbf{p}+\sigma^2)}/\partial p(j)=-\frac{p(i)[\mathbf{D}]_{ii}\mathbf{\Phi}_{ji}}{([\mathbf{D}]_{ii}(\mathbf{\Phi}_i^T\mathbf{p}+\sigma^2))^2}<0$. If we slightly reduce $p(n_1)$ by δ, then we can obtain a new power assignment vector denoted as $\hat{\mathbf{p}}$ which ensures $\frac{\hat{p}_1(n_1)}{[\mathbf{D}]_{n_1n_1}(\mathbf{\Phi}_{n_1}^T\hat{\mathbf{p}}_1+\sigma^2)}\geq\gamma^*$.

On the other hand, as $p(n_1)$ decreases, we have $\frac{\hat{p}_1(i)}{[\mathbf{D}]_{ii}(\mathbf{\Phi}_i^T\hat{\mathbf{p}}_1+\sigma^2)}>\gamma^*,\ \forall i\neq n_1$. Namely, the minimum of all weighted SINR is not reduced when the total consumed power reduces as $\mathbf{1}^T\hat{\mathbf{p}}_1=\mathbf{1}^T\mathbf{p}_{max}-\delta$. Hence, as we have proved in the above part, by re-distributing δ, we can definitely obtain an increasing in threshold $\hat{\gamma}^*$ with $\hat{\gamma}^*>\gamma^*$. This contradicts to our assumption. ■

APPENDIX B
PROOF OF LEMMA 1

Proof: Given the definition of cost function $\tilde{\lambda}(\mathbf{G},\mathbf{p})$, for arbitrary $\mathbf{G}$ and $\mathbf{p}$, it can also be formulated as $\tilde{\lambda}(\mathbf{G},\mathbf{p})=\max_{i=1,\ldots,K+1}\frac{\mathbf{e}_i^T\mathbf{\Lambda}(\mathbf{G})\tilde{\mathbf{p}}}{\mathbf{e}_i^T\tilde{\mathbf{p}}}$, where $\mathbf{e}_i$ is a column vector with i^{th} element being one and the rest being zero [28]. From this it follows:

$$\mathbf{e}_i^T\tilde{\mathbf{p}}=\begin{cases}p(i) & ,i\leq K\\ 1 & ,i=K+1\end{cases},\text{ and}$$

$$\mathbf{e}_i^T\mathbf{\Lambda}(\mathbf{G})\tilde{\mathbf{p}}=\begin{cases}\frac{\gamma_i}{SINR_i^{UL}} & ,i\leq K\\ \frac{1}{P_{total}}\sum_{i=1}^{K}\frac{\gamma_i p(i)}{SINR_i^{UL}} & ,i=K+1.\end{cases}$$

It can be easily verified that $\frac{1}{P_{total}}\sum_{i=1}^{K}\frac{\gamma_i p(i)}{SINR_i^{UL}}\leq\max_i\frac{\gamma_i}{SINR_i^{UL}}$ and $\frac{1}{P_{total}}\sum_{i=1}^{K}\frac{\gamma_i p(i)}{SINR_i^{UL}}\geq\min_i\frac{\gamma_i}{SINR_i^{UL}}$. Thus we have $\tilde{\lambda}(\mathbf{G},\mathbf{p})=\max_{i=1,\ldots,K+1}\frac{\mathbf{e}_i^T\mathbf{\Lambda}(\mathbf{G})\tilde{\mathbf{p}}}{\mathbf{e}_i^T\tilde{\mathbf{p}}}=\max_{i=1,\ldots,K}\frac{\gamma_i}{SINR_i^{UL}(\mathbf{G},\mathbf{p})}$, and $\min_{\mathbf{x}>\mathbf{0}}\frac{\mathbf{x}^T\mathbf{\Lambda}(\mathbf{G},P_{total})\tilde{\mathbf{p}}}{\mathbf{x}^T\tilde{\mathbf{p}}}=\min_{i=1,\ldots,K+1}\frac{\mathbf{e}_i^T\mathbf{\Lambda}(\mathbf{G})\tilde{\mathbf{p}}}{\mathbf{e}_i^T\tilde{\mathbf{p}}}=\min_{i=1,\ldots,K}\frac{\gamma_i}{SINR_i^{UL}(\mathbf{G},\mathbf{p})}$ which will be used in the next section in appendix.

For a given $\mathbf{p}_{ary}$, it can be derived that $\tilde{\lambda}(\mathbf{G},\tilde{\mathbf{p}}_{ary})=\max_{i=1,\ldots,K}\frac{\gamma_i}{SINR_i^{UL}(\mathbf{G},\mathbf{p}_{ary})}$, and the corresponding optimal signature matrix $\mathbf{G}^*$ with fixed power assignment can be obtained by $\mathbf{G}^*=\arg\min_{\mathbf{G}}\max_{i=1,\ldots,K}\frac{\gamma_i}{SINR_i^{UL}(\mathbf{G},\mathbf{p}_{ary})}$. Given a power assignment vector $\mathbf{p}_{ary}$, since the uplink SINR for each user only depends on $\mathbf{g}_i$ and is independent of $\mathbf{g}_j, i\neq j$, $\mathbf{g}_i^*=\arg\min_{\|\mathbf{g}_i\|_2=1}\frac{\gamma_i}{SINR_i^{UL}(\mathbf{G},\mathbf{p}_{ary})}$. ■

APPENDIX C
PROOF OF THEOREM 2

Proof: Here, we prove the necessary and sufficient condition in Theorem 2 by contradiction.

1) To prove the sufficiency: suppose $\mathbf{G}^*$ is not the global optimizer of the problem in (9), where $\mathbf{G}^*=\arg\min_{\|\mathbf{g}_i\|_2=1,\forall i}\tilde{\lambda}(\mathbf{G},\mathbf{p}^*)$ and $\tilde{\mathbf{p}}^*=[\mathbf{p}^*,\ 1]$ is the dominant eigenvector of $\mathbf{\Lambda}(\mathbf{G}^*,P_{total})$.
Suppose there exists another $\hat{\mathbf{G}}$ such that $\lambda_{max}(\mathbf{\Lambda}(\hat{\mathbf{G}},P_{total}))<\lambda_{max}(\mathbf{\Lambda}(\mathbf{G}^*,P_{total}))$. Recall (10) we can have

$$\begin{aligned}\gamma_{global}^{-1}&=\lambda_{max}(\mathbf{\Lambda}(\hat{\mathbf{G}},P_{total}))\\&=\min_{\mathbf{G}}\lambda_{max}(\mathbf{\Lambda}(\mathbf{G},P_{total}))\\&=\min_{\mathbf{G}}\min_{\mathbf{x}>\mathbf{0}}\max_{\mathbf{y}>\mathbf{0}}\frac{\mathbf{x}^T\mathbf{\Lambda}(\mathbf{G},P_{total})\mathbf{y}}{\mathbf{x}^T\mathbf{y}}\\&\geq\min_{\mathbf{G}}\min_{\mathbf{x}>\mathbf{0}}\frac{\mathbf{x}^T\mathbf{\Lambda}(\mathbf{G},P_{total})\tilde{\mathbf{p}}^*}{\mathbf{x}^T\tilde{\mathbf{p}}^*}\\&=\min_{\mathbf{G}}\min_i\frac{\gamma_i}{SINR_i^{UL}(\mathbf{G},\mathbf{p}^*)}\\&=\min_i\frac{\gamma_i}{SINR_i^{UL}(\mathbf{G}^*,\mathbf{p}^*)}\\&=\lambda_{max}(\mathbf{\Lambda}(\mathbf{G}^*,P_{total})).\end{aligned}\tag{19}$$

In (19), we have $\lambda_{max}(\mathbf{\Lambda}(\hat{\mathbf{G}},P_{total}))\geq\lambda_{max}(\mathbf{\Lambda}(\mathbf{G}^*,P_{total}))$, which contradicts to that $\hat{\mathbf{G}}$ is the global optimum.

2) To prove the necessity: suppose $\mathbf{G}^*$ is the global optimizer with the corresponding power vector being $\mathbf{p}^*$ and $\tilde{\lambda}(\mathbf{G}^*, \mathbf{p}^*) > \min_{\mathbf{G}} \tilde{\lambda}(\mathbf{G}, \mathbf{p}^*)$. Moreover, suppose there exists an arbitrary feasible $\tilde{\mathbf{G}}$ that satisfies $\tilde{\lambda}(\tilde{\mathbf{G}}, \mathbf{p}^*) = \min_{\mathbf{G}} \tilde{\lambda}(\mathbf{G}, \mathbf{p}^*)$, i.e. $\tilde{\lambda}(\mathbf{G}^*, \mathbf{p}^*) > \tilde{\lambda}(\tilde{\mathbf{G}}, \mathbf{p}^*)$.
Since $\mathbf{G}^*$ is the global optimizer, we have

$$\begin{aligned}
&\tilde{\lambda}(\mathbf{G}^*, \mathbf{p}^*) = \lambda_{max}(\mathbf{\Lambda}(\mathbf{G}^*, P_{total})) \\
&= \min_{\mathbf{G}} \lambda_{max}(\mathbf{\Lambda}(\mathbf{G}, P_{total})) \leq \lambda_{max}(\mathbf{\Lambda}(\tilde{\mathbf{G}}, P_{total})) \\
&= \min_{\mathbf{y}\succ\mathbf{0}} \max_{\mathbf{x}\succ\mathbf{0}} \frac{\mathbf{x}^T \mathbf{\Lambda}(\tilde{\mathbf{G}}, P_{total})\mathbf{y}}{\mathbf{x}^T\mathbf{y}} \\
&\leq \max_{\mathbf{x}\succ\mathbf{0}} \frac{\mathbf{x}^T \mathbf{\Lambda}(\tilde{\mathbf{G}}, P_{total})\tilde{\mathbf{p}}^*}{\mathbf{x}^T\tilde{\mathbf{p}}^*} = \tilde{\lambda}(\tilde{\mathbf{G}}, \mathbf{p}^*). \qquad (20)
\end{aligned}$$

Then we have $\tilde{\lambda}(\mathbf{G}^*, \mathbf{p}^*) \leq \tilde{\lambda}(\tilde{\mathbf{G}}, \mathbf{p}^*)$, which contradicts to the assumption. ■

APPENDIX D
PROOF OF THEOREM 3

Proof: According to the definition of cost function, we have

$$\begin{aligned}
\tilde{\lambda}(\mathbf{G}^{(n+1)}, \mathbf{p}^{(n)}) &= \min_{\|\mathbf{g}_i\|_2=1, \forall i} \tilde{\lambda}(\mathbf{G}, \mathbf{p}^{(n)}) \\
&\leq \tilde{\lambda}(\mathbf{G}^{(n)}, \mathbf{p}^{(n)}) = \lambda_{max}^{(n)}. \qquad (21)
\end{aligned}$$

Moreover, we also have

$$\begin{aligned}
\lambda_{max}^{(n+1)} &= \min_{\mathbf{p}\succ 0} \tilde{\lambda}(\mathbf{G}^{(n+1)}, \mathbf{p}) \\
&= \min_{\tilde{\mathbf{p}}\succ 0} \max_{\mathbf{x}\succ 0} \frac{\mathbf{x}^T \mathbf{\Lambda}(\mathbf{G}^{(n+1)},\ P_{total})\tilde{\mathbf{p}}}{\mathbf{x}^T\tilde{\mathbf{p}}} \\
&\leq \max_{\mathbf{x}\succ 0} \frac{\mathbf{x}^T \mathbf{\Lambda}(\mathbf{G}^{(n+1)},\ P_{total})\tilde{\mathbf{p}}^{(n)}}{\mathbf{x}^T\tilde{\mathbf{p}}^{(n)}} \\
&= \tilde{\lambda}(\mathbf{G}^{(n+1)}, \mathbf{p}^{(n)}). \qquad (22)
\end{aligned}$$

Combining (21) and (22), it can be induced that $\lambda_{max}^{(n+1)} \leq \lambda_{max}^{(n)}$, $\forall n$. The sequence $\{\lambda_{max}^{(n)}\}$ is nonnegative, lower-bounded by zero, and monotonically decreasing. Hence, the limit $\lambda_{max}^{\infty} = \lim_{n\to\infty} \lambda_{max}^{(n)}$ exists.

So far it has been verified that λ_{max}^{∞} exists, we need to prove that the generated sequence $\{\lambda_{max}^{(n)}\}$ always converges to the global optimum no matter what the initial point is.

Let us denote set $X = \{\mathbf{G} \in \mathbb{C}^{L\times K} : \mathbf{G} = [\mathbf{g}_1, \ldots, \mathbf{g}_K], \|\mathbf{g}_i\|_2 = 1, \forall i\}$, where K is the number of users and L is the channel length. Similarly, $Y = \{\mathbf{p} \in \mathbb{R}_+^K : \|\mathbf{p}\|_1 = P_{total}\}$. Both sets X and Y are convex compact sets, i.e. bounded and closed. Moreover, set $S = \{\lambda_{max} : \lambda_{max} = \rho(\mathbf{\Lambda}(\mathbf{G}, P_{total})), \mathbf{G} \in X\}$ is also compact, due to the compactness of X and the continuity of operator $\rho(\cdot)$ and $\mathbf{\Lambda}(\cdot, P_{total})$. In the algorithm, the tuple $(\mathbf{G}^{(n)}, \mathbf{p}^{(n)})$ is updated in each loop as $(\mathbf{G}^{(n)}, \mathbf{p}^{(n)}) = \mathfrak{T}\{(\mathbf{G}^{(n-1)}, \mathbf{p}^{(n-1)})\}$. The continuous mapping function $\mathfrak{T}$, on the compact space $X \times Y$, is defined as

$$\mathbf{g}_i^{(n)} = \arg \max_{\|\mathbf{g}_i\|_2=1} \frac{SINR_i^{UP}(\mathbf{G}, \mathbf{p}^{(n-1)})}{\gamma_i}, \forall i \qquad (23)$$

$$\lambda_{max}^{(n)} \widetilde{\mathbf{p}}^{(n)} = \mathbf{\Lambda}(\mathbf{G}^{(n)}, P_{total})\widetilde{\mathbf{p}}^{(n)}, \qquad (24)$$

where $\lambda_{max}^{(n)} = \rho(\mathbf{\Lambda}(\mathbf{G}^{(n)}, P_{total}))$, $\mathbf{G} = [\mathbf{g}_1, \ldots, \mathbf{g}_K]$, and augmented vector $\widetilde{\mathbf{p}}^{(n)} = [\mathbf{p}^{(n)}, 1]$. According to the Schauders fixed point theorem, function $\mathfrak{T}$ has at least one fixed point on $X \times Y$, i.e., $\exists(\mathbf{G}^{(\infty)}, \mathbf{p}^{(\infty)})$ such that $(\mathbf{G}^{(\infty)}, \mathbf{p}^{(\infty)}) = \mathfrak{T}\{(\mathbf{G}^{(\infty)}, \mathbf{p}^{(\infty)})\}$. Moreover, the generated sequence $\{\lambda_{max}^{(n)}\}$ is monotonically decreasing and $\lambda_{max}^{(\infty)} = \rho(\mathbf{\Lambda}(\mathbf{G}^{(\infty)}, P_{total}))$.

For every potential fixed point $(\mathbf{G}^{(\infty)}, \mathbf{p}^{(\infty)}, \lambda_{max}^{(\infty)})$, it satisfies both sides of (23), (24) and

$$\lambda_{max}^{(\infty)} \widetilde{\mathbf{p}}^{(\infty)} = \rho(\mathbf{\Lambda}(\mathbf{G}^{(\infty)}, P_{total}))\widetilde{\mathbf{p}}^{(\infty)}. \qquad (25)$$

Moreover, as we have proved in Lemma 1 that $\mathbf{G}^{(\infty)} = \arg \max_{\|\mathbf{g}_i\|_2=1} \frac{SINR_i^{UP}(\mathbf{G}, \mathbf{p}^{(\infty)})}{\gamma_i}$ $\forall i$ is equivalent to $\mathbf{G}^{(\infty)} = \arg \min_{\|\mathbf{g}_i\|_2=1} \frac{\gamma_i}{SINR_i^{UP}(\mathbf{G}, \mathbf{p}^{(\infty)})} = \arg \min_{\|\mathbf{g}_i\|_2=1} \tilde{\lambda}(\mathbf{G}^{(\infty)}, \mathbf{p}^{(\infty)})$. Hence, this tuple satisfies the necessary and sufficient condition in Theorem 2 for the global optimality of joint optimization problem under total power constraint, and thus each locally optimal tuple $(\mathbf{G}^{(\infty)}, \mathbf{p}^{(\infty)}, \lambda_{max}^{(\infty)})$ is indeed a globally optimal tuple to the relaxed problem that $\lambda_{max}^{(\infty)} = \lambda_{max}^{\infty}$. ■

APPENDIX E
PROOF OF LEMMA 2

Proof: Let the optimal power assignment vector in (6) with P_{total} be $\mathbf{p}_0$ and the one with $P_{total} + \Delta(\Delta > 0)$ be $\mathbf{p}_1$. Suppose $\exists n_0$ such that the optimal power assignment $p_0(n_0) \geq p_1(n_0)$ and for other users $p_0(i) < p_1(i)$.

As shown in the proof of Theorem 1 in APPENDIX A, γ^* is a strictly increasing function in P_{total}, i.e., $\gamma_0^* < \gamma_1^*$, where γ_0^* is the optimum under P_{total} and γ_1^* under $P_{total} + \Delta$.

However, as shown in APPENDIX A, $SINR_i^{UL}$ is strictly increasing in $p(i)$ and decreasing in $p(j)$, $\forall j \neq i$. This gives us that $SINR_{0,n_0}^{UL} \geq SINR_{1,n_0}^{UL}$, where $SINR_{0,n_0}^{UL}$ is the SINR of n_0^{th} user under P_{total} and $SINR_{1,n_0}^{UL}$ is the one under $P_{total} + \Delta$.

According to Theorem 1, we have $SINR_{0,n_0}^{UL}/\gamma_{n_0} = \gamma_0^*$ and $SINR_{1,n_0}^{UL}/\gamma_{n_0} = \gamma_1^*$. This implies that $\gamma_0^* \geq \gamma_1^*$, which contradicts to the assumption. ■

APPENDIX F
PROOF OF THEOREM 4

Proof: In the initialization, as $P_{total}^{(0)} = \mathbf{1}^T\mathbf{P}_{max}$ is an extreme case in our SINR balancing problem, $\delta^{(0)}$ is usually smaller than 0. Except when $\delta^{(0)} = 0$ wherein the optimal power assignment is equal to each individual constraints, our algorithm terminates.

At the n^{th} iteration, if the $\delta^{(n)} > 0$, we use backward search with a coefficient $0 < \eta < 1$ to adjust the stepsize δP_{total} without flip its direction. As a result, we can make sure at the end of n^{th} iteration $\delta^{(n)} < 0$ and the relaxed feasible set is tightened. The stepsize for gradient search is defined as $\delta P_{total} = \frac{\delta^{(n-1)}}{\text{slope}}$, where slope $= \frac{p^{(n-1)}(\text{index}) - p(\text{index})}{(1-\mu)P_{total}^{(n-1)}}$. According to Lemma 2, the slope is always positive since $\mathbf{p}$ is the optimal power assignment vector with $\mu P_{total}^{(n-1)}$ and $0 < \mu < 1$ is a predefined coefficient. Since $\delta^{(n-1)}$ is always less than or equal to 0 in the proposed algorithm, we have stepsize $\delta P_{total} \leq 0$ at the n^{th} iteration, implying $P_{total}^{(n)} = P_{total}^{(n-1)} + \delta P_{total} \leq P_{total}^{(n-1)}$ and $\mathbf{p}^{(n)} \preceq \mathbf{p}^{(n-1)}$. Hence, $\delta^{(n)} = \min_i \{p_{max}(i) - p^{(n)}(i)\} \geq \delta^{(n-1)}$. Moreover, the equality holds if and only if $\delta^{(n-1)} = 0$. As a consequence, the sequence $\{\delta^{(n)}\}_{n=1}^{\infty}$ is a nonpositive, monotonically increasing sequence and upper-bounded by 0. The limit exists and $\lim_{n\to\infty} \delta^{(n)} = \delta^{\infty} \leq 0$.

Suppose $\delta^{\infty} = \mu < 0$ and it is achieved for some n_0, i.e. $\delta^{(n)} = \mu$, $\forall\, n \geq n_0$. Then from Alrotighm 2, we have $P_{total}^{(n_0+1)} = P_{total}^{(n_0)} + \delta P_{total} \leq P_{total}^{(n_0)}$. As an immediate result $0 \geq \delta^{(n_0+1)} > \delta^{(n_0)} = \mu$, which contradicts to the assumption that the sequence converges to μ. Thus, the limit point of $\{\delta^{(n)}\}_{n=1}^{\infty}$ is $\delta^{\infty} = 0$.

Hence, since the sequence $\{\delta^{(n)}\}_{n=1}^{\infty}$ is strictly increasing before converging and the limit of $\{\delta^{(n)}, n = 1, 2, \ldots\}$ is $\delta^{\infty} = 0$. Our algorithm will converge to the global optimum. ■

Appendix G
Explanation for Assumption 1

To simplify the analysis, let us consider the noise variance $\sigma^2 = 1$. When the constraint is P_{total}, we can have our $\mathbf{g}_i^{MMSE}$ calculated as shown in (26).

$$\begin{aligned}\mathbf{g}_i^{MMSE} &= c_i \left(\sum_j p(j)\mathbf{R}_j + \sigma^2\mathbf{I}\right)^{-1} \mathbf{H}_i^{(L)H} \\ &= c_i \mathbf{B}^{-1}(\mathbf{k})\mathbf{H}_i^{(L)H}\frac{1}{P_{total}}. \end{aligned} \tag{26}$$

With a slightly perturbation Δ, the updated version of $\mathbf{g}_i^{MMSE}$ is defined as

$$\begin{aligned}&\mathbf{g}_{\Delta i}^{MMSE} \\ &= \tilde{c}_i \left(\sum_j p(j)\mathbf{R}_j + \sum_j \delta p(j)\mathbf{R}_j + \sigma^2\mathbf{I}\right)^{-1} \mathbf{H}_i^{(L)H} \\ &= \tilde{c}_i \left(\sum_j k_j\mathbf{R}_j + \frac{1}{P_{total}}\mathbf{I} + \frac{\sum_j \delta p(j)\mathbf{R}_j}{P_{total}}\right)^{-1} \mathbf{H}_i^{(L)H}\frac{1}{P_{total}} \\ &= \frac{\tilde{c}_i}{c_i}\mathbf{g}_i^{MMSE} + \frac{\tilde{c}_i}{c_i}\sum_{n\geq 1}\left(-\frac{\sum_j \delta p(j)\mathbf{R}_j\mathbf{B}^{-1}(\mathbf{k})}{P_{tota}}\right)^n \mathbf{g}_i^{MMSE}. \end{aligned} \tag{27}$$

Then, the difference between $\mathbf{g}_i^{MMSE}$ and $\mathbf{g}_{\Delta i}^{MMSE}$ can be denoted as $\delta\mathbf{g}_i^{MMSE}$ in (28).

$$\begin{aligned}\delta\mathbf{g}_i^{MMSE} = &\sum_{m\geq 1}\left(\frac{\sum_j \delta p(j)\mathbf{R}_j\mathbf{B}^{-1}(\mathbf{k})}{P_{tota}}\right)^{2m-1} \\ &\times\left(\frac{\sum_j \delta p(j)\mathbf{R}_j\mathbf{B}^{-1}(\mathbf{k})}{P_{tota}} - \mathbf{I}\right)\mathbf{g}_i^{MMSE}. \end{aligned} \tag{28}$$

As $\Delta < 10^{-2}$ and $\|\mathbf{g}_i^{MMSE}\|_2 = 1$, we can derive a bound for $\|\delta\mathbf{g}_i^{MMSE}\|_2$ as

$$\begin{aligned}\left\|\delta\mathbf{g}_i^{MMSE}\right\|_2 \leq &\left\|\sum_{m\geq 1}\left(\frac{\sum_j \delta p(j)\mathbf{R}_j\mathbf{B}^{-1}(\mathbf{k})}{P_{total}}\right)^{2m-1}\right. \\ &\left.\times\left(\frac{\sum_j \delta p(j)\mathbf{R}_j\mathbf{B}^{-1}(\mathbf{k})}{P_{total}} - \mathbf{I}\right)\right\|_2 \\ \leq &\sum_{m\geq 1}\left\|\frac{\sum_j \delta p(j)\mathbf{R}_j\mathbf{B}^{-1}(\mathbf{k})}{P_{total}}\right\|_2^{2m-1} \\ &\times\left\|\frac{\sum_j \delta p(j)\mathbf{R}_j\mathbf{B}^{-1}(\mathbf{k})}{P_{total}} - \mathbf{I}\right\|_2. \end{aligned} \tag{29}$$

Moreover, as we define $\tilde{k}(i) = \frac{\delta p(i)}{\Delta}$ and $\Delta < 10^{-2}$, we assume $\tilde{k}(i)\Delta \approx k(i)\Delta$. Then we can have

$$\begin{aligned}&\frac{\sum_j \delta p(j)\mathbf{R}_j\mathbf{B}^{-1}(\mathbf{k})}{P_{total}} = \Delta\sum_j \tilde{k}(j)\mathbf{R}_j\mathbf{B}^{-1}(\mathbf{k}) \\ &\approx \Delta\sum_j k(j)\mathbf{R}_j\mathbf{B}^{-1}(\mathbf{k}) = \Delta\mathbf{B}^{-1}(\mathbf{k})\left(\mathbf{B}(\mathbf{k}) - \frac{1}{P_{total}}\mathbf{I}\right) \\ &= \Delta\left(\mathbf{I} - \frac{1}{P_{total}}\mathbf{B}^{-1}(\mathbf{k})\right). \end{aligned} \tag{30}$$

Since the eigenvalues of $\frac{1}{P_{total}}\mathbf{B}^{-1}(\mathbf{k})$ lie in (0, 1), the eigenvalues of $\frac{\sum_j \delta p(j)\mathbf{R}_j\mathbf{B}^{-1}(\mathbf{k})}{P_{total}}$ will lie in $(0, \Delta)$. As a result, $\|\frac{\sum_j \delta p(j)\mathbf{R}_j\mathbf{B}^{-1}(\mathbf{k})}{P_{total}}\|_2 < \Delta$ and $\|\frac{\sum_j \delta p(j)\mathbf{R}_j\mathbf{B}^{-1}(\mathbf{k})}{P_{total}} - \mathbf{I}\|_2 < 1$, which implies $\|\delta\mathbf{g}_i^{MMSE}\|_2 < \sum_{m\geq 1}\Delta^{2m-1} = \frac{\Delta}{1-\Delta^2} \simeq \Delta$. Hence, under a small perturbation in P_{total}, the optimal signature matrix can be approximately viewed as unchanging.

References

[1] A. Goldsmith, *Wireless Communications*. Cambridge, U.K.: Cambridge Univ. Press, 2005.

[2] B. Wang, Y. Wu, F. Han, Y.-H. Yang, and K. Liu, "Green wireless communications: A time-reversal paradigm," *IEEE J. Sel. Areas Commun.*, vol. 29, no. 8, pp. 1698–1710, Sep. 2011.

[3] F. Han, Y.-H. Yang, B. Wang, Y. Wu, and K. Liu, "Time-reversal division multiple access over multi-path channels," *IEEE Trans. Commun.*, vol. 60, no. 7, pp. 1953–1965, Jul. 2012.

[4] Y. Chen, Y.-H. Yang, F. Han, and K. R. Liu, "Time-reversal wideband communications," *IEEE Signal Process. Lett.*, vol. 20, no. 12, pp. 1219–1222, Dec. 2013.

[5] Y. Chen *et al.*, "Time-reversal wireless paradigm for green internet of things: An overview," *IEEE Internet Things J.*, vol. 1, no. 1, pp. 81–98, Feb. 2014.

[6] Y.-H. Yang, B. Wang, W. S. Lin, and K. R. Liu, "Near-optimal waveform design for sum rate optimization in time-reversal multiuser downlink systems," *IEEE Trans. Wireless Commun.*, vol. 12, no. 1, pp. 346–357, Jan. 2013.

[7] M. Fink, C. Prada, F. Wu, and D. Cassereau, "Self focusing in inhomogeneous media with time reversal acoustic mirrors," in *Proc. IEEE Ultrason. Symp.*, 1989, pp. 681–686.
[8] M. Fink, "Time reversal of ultrasonic fields. I. Basic principles," *IEEE Trans. Ultrason. Ferroelectr. Freq. Control*, vol. 39, no. 5, pp. 555–566, Sep. 1992.
[9] F. Wu, J.-L. Thomas, and M. Fink, "Time reversal of ultrasonic fields. II. Experimental results," *IEEE Trans. Ultrason. Ferroelectr. Freq. Control*, vol. 39, no. 5, pp. 567–578, Sep. 1992.
[10] W. Kuperman, W. S. Hodgkiss, H. C. Song, T. Akal, C. Ferla, and D. R. Jackson, "Phase conjugation in the ocean: Experimental demonstration of an acoustic time-reversal mirror," *J. Acoust. Soc. Amer.*, vol. 103, no. 1, pp. 25–40, 1998.
[11] D. Rouseff, D. R. Jackson, W. L. Fox, C. D. Jones, J. A. Ritcey, and D. R. Dowling, "Underwater acoustic communication by passive-phase conjugation: Theory and experimental results," *IEEE J. Ocean. Eng.*, vol. 26, no. 4, pp. 821–831, Oct. 2001.
[12] G. Lerosey, J. De Rosny, A. Tourin, A. Derode, G. Montaldo, and M. Fink, "Time reversal of electromagnetic waves and telecommunication," *Radio Sci.*, vol. 40, no. 6, pp. 1–10, 2005.
[13] G. Lerosey, J. De Rosny, A. Tourin, A. Derode, and M. Fink, "Time reversal of wideband microwaves," *Appl. Phys. Lett.*, vol. 88, no. 15, p. 154101, 2006.
[14] M. Emami, M. Vu, J. Hansen, A. J. Paulraj, and G. Papanicolaou, "Matched filtering with rate back-off for low complexity communications in very large delay spread channels," *in Proc. 38th Asilomar Conf. Signals Syst. Comput.*, 2004, pp. 218–222.
[15] J. de Rosny, G. Lerosey, and M. Fink, "Theory of electromagnetic time-reversal mirrors," *IEEE Trans. Antennas Propag.*, vol. 58, no. 10, pp. 3139–3149, Oct. 2010.
[16] T. S. Rappaport, *Wireless Communications: Principles and Practice*. Piscataway, NJ, USA: IEEE Press, 1996.
[17] J. Zander, "Performance of optimum transmitter power control in cellular radio systems," *IEEE Trans. Veh. Technol.*, vol. 41, no. 1, pp. 57–62, Feb. 1992.
[18] S. A. Grandhi, R. Vijavan, D. J. Goodman, and J. Zander, "Centralized power control in cellular radio systems," *IEEE Trans. Veh. Technol.*, vol. 42, no. 4, pp. 466–468, Nov. 1993.
[19] R. D. Yates, "A framework for uplink power control in cellular radio systems," *IEEE J. Sel. Areas Commun.*, vol. 13, no. 7, pp. 1341–1347, Sep. 1995.
[20] A. Sampath, S. P. Kumar, and J. M. Holtzman, "Power control and resource management for a multimedia CDMA wireless system," *in Proc. 6th Int. Symp. Pers. Indoor Mobile Radio Commun.*, 1995, pp. 21–25.
[21] T. Alpcan, T. Başar, R. Srikant, and E. Altman, "CDMA uplink power control as a noncooperative game," *Wireless Netw.*, vol. 8, no. 6, pp. 659–670, 2002.
[22] D. Gerlach and A. Paulraj, "Base station transmitting antenna arrays for multipath environments," *Signal Process.*, vol. 54, no. 1, pp. 59–73, 1996.
[23] F. Rashid-Farrokhi, K. Liu, and L. Tassiulas, "Transmit beamforming and power control for cellular wireless systems," *IEEE J. Sel. Areas Commun.*, vol. 16, no. 8, pp. 1437–1450, Oct. 1998.
[24] E. Visotsky and U. Madhow, "Optimum beamforming using transmit antenna arrays," in *Proc. IEEE 49th Veh. Technol. Conf.*, 1999, pp. 851–856.
[25] D. N. Tse and P. Viswanath, "Downlink-uplink duality and effective bandwidths," in *Proc. IEEE Int. Symp. Inf. Theory*, 2002, p. 52.
[26] H. Boche and M. Schubert, "A general duality theory for uplink and downlink beamforming," in *Proc. IEEE Veh. Technol. Conf.*, 2002, pp. 87–91.
[27] W. Yang and G. Xu, "Optimal downlink power assignment for smart antenna systems," in *Proc. IEEE Int. Conf. Acoust. Speech Signal Process.*, 1998, pp. 3337–3340.
[28] M. Schubert and H. Boche, "Solution of the multiuser downlink beamforming problem with individual SINR constraints," *IEEE Trans. Veh. Technol.*, vol. 53, no. 1, pp. 18–28, Jan. 2004.
[29] M. Schubert and H. Boche, "Iterative multiuser uplink and downlink beamforming under SINR constraints," *IEEE Trans. Signal Process.*, vol. 53, no. 7, pp. 2324–2334, Jul. 2005.
[30] Z. Shen, J. G. Andrews, and B. L. Evans, "Adaptive resource allocation in multiuser OFDM systems with proportional rate constraints," *IEEE Trans. Wireless Commun.*, vol. 4, no. 6, pp. 2726–2737, Nov. 2005.
[31] D. W. Cai, T. Q. Quek, and C. W. Tan, "Coordinated max-min SIR optimization in multicell downlink-duality and algorithm," in *Proc. IEEE Int. Conf. Commun.*, 2011, pp. 1–6.
[32] D. W. Cai, C. W. Tan, and S. H. Low, "Optimal max-min fairness rate control in wireless networks: Perron-Frobenius characterization and algorithms," *in Proc. INFOCOM*, 2012, pp. 648–656.
[33] Y. Huang, C. W. Tan, and B. Rao, "Joint beamforming and power control in coordinated multicell: Max-min duality, effective network and large system transition," *IEEE Trans. Wireless Commun.*, vol. 12, no. 6, pp. 2730–2742, Jun. 2013.
[34] E. Seneta, *Non-Negative Matrices and Markov Chains*. New York, NY, USA: Springer, 2006.
[35] A. Arkhangel'Skii, V. Fedorchuk, D. O'Shea, and L. Pontryagin, *General Topology I: Basic Concepts and Constructions Dimension Theory*. New York, NY, USA: Springer, 2012, vol. 17.
[36] C. W. Tan, M. Chiang, and R. Srikant, "Maximizing sum rate and minimizing MSE on multiuser downlink: Optimality, fast algorithms and equivalence via max-min SINR," *IEEE Trans. Signal Process.*, vol. 59, no. 12, pp. 6127–6143, Dec. 2011.
[37] D. W. Cai, T. Q. Quek, and C. W. Tan, "A unified analysis of max-min weighted SINR for MIMO downlink system," *IEEE Trans. Signal Process.*, vol. 59, no. 8, pp. 3850–3862, Aug. 2011.
[38] D. W. Cai, T. Q. Quek, C. W. Tan, and S. H. Low, "Max-min SINR coordinated multipoint downlink transmission—Duality and algorithms," *IEEE Trans. Signal Process.*, vol. 60, no. 10, pp. 5384–5395, Oct. 2012.
[39] S. Friedland *et al.*, "Some inequalities for the spectral radius of nonnegative matrices and applications," *Duke Math. J*, vol. 42, no. 3, pp. 459–490, 1975.

Qinyi Xu (S'15) received the B.S. degree (highest Hons.) in information engineering from the Southeast University, Nanjing, China, in 2013. She is currently pursuing the Ph.D. degree in the electrical and computer engineering at the University of Maryland, College Park, MD, USA. She was an exchange student at KTH-Royal Institute of Technology, Stockholm, Sweden from August 2012 to January 2013, with the National Sponsorship of China. Her research interests include signal processing and wireless communications. She was the recipient of the Clark School Distinguished Graduate Fellowships from the University of Maryland, and the Graduate with Honor Award from the Southeast University in 2013.

Yan Chen (SM'14) received the Bachelor's degree from the University of Science and Technology, Hefei, China, the M. Phil degree from Hong Kong University of Science and Technology (HKUST), Clear Water Bay, Hong Kong, and the Ph.D. degree from University of Maryland, College Park, MD, USA, in 2004, 2007, and 2011, respectively. His research interests data science, network science, game theory, social learning and networking, and signal processing and wireless communications. He was the recipient of multiple honors and awards including the Best Paper Award from IEEE GLOBECOM in 2013, Future Faculty Fellowship and Distinguished Dissertation Fellowship Honorable Mention from the Department of Electrical and Computer Engineering in 2010 and 2011, Finalist of the Dean's Doctoral Research Award from A. James Clark School of Engineering, University of Maryland, in 2011, and the Chinese Government Award for outstanding students abroad in 2011.

K. J. Ray Liu (F'03) was a Distinguished Scholar-Teacher with the University of Maryland, College Park, MD, USA, in 2007, where he is Christine Kim Eminent Professor of information technology. He leads the Maryland Signals and Information Group conducting research encompassing broad areas of information and communications technology with recent focus on future wireless technologies, network science, and information forensics and security. He was the recipient of the 2016 IEEE Leon K. Kirchmayer Technical Field Award on graduate teaching and mentoring, the IEEE Signal Processing Society 2014 Society Award, and the IEEE Signal Processing Society 2009 Technical Achievement Award. He was recognized by Thomson Reuters as a Highly Cited Researcher and is a Fellow of AAAS. He is a Director-Elect of the IEEE Board of Directors. He was the President of IEEE Signal Processing Society, where he has served as a Vice President of Publications and Board of Governor. He has also served as the Editor-in-Chief of the *IEEE Signal Processing Magazine*. He has received teaching and research recognitions from the University of Maryland including the university-level Invention of the Year Award and the college-level Poole and Kent Senior Faculty Teaching Award, Outstanding Faculty Research Award, and Outstanding Faculty Service Award, all from A. James Clark School of Engineering.